Int. J. Econ. Environ. Geol. Vol. 14 (2) 27-34, 2023
Journal home page: www.econ-environ-geol.org

Open Access
ISSN: 2223-957X

Mapping Alteration Zones for Detection of Economic Minerals using Integrated Tools in District Lower Dir, Northwest Khyber Pakhtunkhwa, Pakistan

Nazir Ul Islam[1], Liu Lei[1], Yasir Shaheen Khalil[1], Said Mukhtar Ahmad[2*], Imran Ullah[2]

[1]School of Earth Sciences & Resources, Chang'an University Xi'an, China
[2] Department of Earth Sciences Quaid I Azam University, Pakistan

* Email: mukhtargeo44@gmail.com

Abstract: The study area is the part of Lower Dir which is geographically situated in the NW of Khyber Pakhtunkhwa province, Pakistan. Geologically this area lies in the western part of the well-known Kohistan Island Arc. It represents the best exposure to subduction-related island arc and has been regarded as the prominent metallogenic belt that hosts a variety of various minerals. The area has experienced various tectonic episodes in the past and altered the rock assemblages which developed the huge potential of copper and other precious base metals. To detect and monitor these alteration zones, remote sensing techniques coupled with field observation were evaluated in the current study. Landsat-7, Landsat-8, and Sentinel-2B images were processed under the shelter of Principal component (Crosta technique) analysis to demarcate the separate alteration zones. It was confirmed from the results that the signature of the mapped alteration zone reflects the ground truth observation of copper mineralization in the target area. Furthermore, remote sensing signatures were correlated with the petrographic details which also confirmed these alteration zones. Spectrometry of the selected samples also delineates the same signature which is best fitted with the remote sensing data. From our current analysis, we suggest that a principal component technique in terms of medium to high-resolution remote sensing data is more beneficial for mineral exploration.

Keywords; Landsat-8, sentinel-2B, principal component analysis, alteration zones.

Introduction

Hydrothermal alteration is the product of the response of former rock forming minerals to physical and chemical conditions different from those, under which they initially formed, particularly by the action of hydrothermal fluids (Pirajno, 1992). Hydrothermal alteration plays a key role in mineral delineation, surrounding the ore body that facilitates and focuses the exploration activity to smaller targets (Abhary and Hassani, 2016). These alteration aureoles are the imaginary basis for mapping zones of alteration during the mineral exploration stage by using remote sensing data (Hunt, 1977; Sabins, 1999). Remote sensing images have been successfully used for mineral exploration since the launch of Landsat in 1972 (Ducart et al., 2016; Safari and Kabir, 2017; Hisham et al., 2017). Remote sensing can delineate and map alteration zone which is exposed on the surface of the earth, especially the inaccessible region. Furthermore, large areas of mineralization can be mapped in short time space and at a comparatively low cost (Mia and Fujimitsu, 2012). Various remote sensing surveys for mineral prospecting have been executed to identify mineral features of hydrothermal alterations including the pinpointing features of iron oxides, carbonate or hydroxyl-bearing minerals (Fraser, 1991; Crosta et al., 1998; Ferrier et al., 2002; Torres-Vera and Prol-Ledesma, 2003; Ranjbar et al., 2004; Cheng et al., 2006; Sadeghi et al 2013). The Landsat-7, Landsat-8, Operational Land Imager (OLI) and Sentinel-2B data are the usually used multispectral datasets for alteration zones mapping (Crosta and Moore, 1989; Fraser, 1991). Moore et al., 2008; Gabr et al 2015; Mars and Rowan, 2010; Liu et al., 2016; Amer et al., 2016).Three groups of minerals such as hydroxyl bearing or carbonate minerals (sericite, kaolinite, chlorite, calcite and illite) (Torres-Vera and Prol-Ledesma, 2003; Pour and Hashim 2015) and iron oxide minerals such as (hematite, goethite and limonite) are used to map alteration with remote sensing data (Sadeghi et al., 2013). In recent years, remote sensing techniques were utilized by various researchers for hydrothermal alteration mapping i.e. (Liu et al., 2013; Ousmanou et la., 2023; Anwar et al., 2023; Sikakwe et al., 2023; Liu et al., 2023; Yousufi et al., 2023).

The Dir area studied in the current work is situated in the Northwestern part of Khyber Pakhtunkhwa and has a great potential for copper mineral deposits. Recently few researchers used remote sensing data to map the lithology and alteration zones in northern areas of Pakistan. Ahmad, (2016), used Landsat-8 and ASTER data for the identification of alteration zones for metallic minerals deposits in Northern Pakistan. ASTER data has been used for mapping the lithology of the Chitral region (Khan and Glenn, 2006). In these studies, principal component analysis (PCA) has been applied to process remote sensing data. However, field inspections revealed that false anomalies (iron oxides, hydroxyl bearing and carbonate minerals) induced by vegetation, cloud, shadow and other factors seriously affected the results (Han et al., 2010; Zhang et al., 2004; Zhang and Zhang, 2007). In this work, we target the Dir area which is still unexplored in terms of new emerging techniques and no previous work is available in this aspect. For this reason we attempts to accomplish complete and accurate information for

discovering prospective alteration zones in target area by integrating multi temporal Landsat-7, Landsat-8, Sentinel-2B, field verification and laboratory analysis datasets. The research area is part of the Higher Himalayas lying between longitude $71^0$35'to $71^0$55' E and latitude $35^0$01' to $34^0$55' N on the Survey of Pakistan Topo sheet No. 38 N/9 and 38 N/13 (Fig. 1). The investigated area covers the northwestern part of the Kohistan Island Arc which is nearly in contact with Main Mantle Thrust. Kohistan Island Arc (KIA) is bounded by Main Karakorum Thrust (MKT) in the north and Main Mantle Thrust (MMT) in the south (Tahirkheli, 1979; Treloar and Izatt, 1993; Bignold and Treloar, 2003).

The whole region of the project area is comprised of igneous and metamorphic complexes. These complexes mainly include the rocks of Kamila amphibolite's, Deshi dolerites and Dir group rocks (Fig. 1). The amphibolite's sequence underlain the rocks of the Dir group, a thick succession of calc-alkaline, meta-volcanics in the upper part whereas meta-sediments in the lower part of the selected region (Treloar and Izatt, 1993). The meta-sediments, known as Baraual Banda meta-sediments, are mostly phyllite, pebbly sandstone, slates, and thin beds of limestone of early Eocene age (Tahirkheli, 1982). The meta-volcanic, known as Utror-volcanic mostly comprises basalt, basaltic-andesitic and andesite (Shah and Shervais, 1999). These volcanics have upper faulted contact with Kohistan batholiths and lower faulted contact along Dir Thrust with Baraual Banda Formation (Coward et al., 1986; Sullivan et al., 1993; Ahmed et al., 2000).

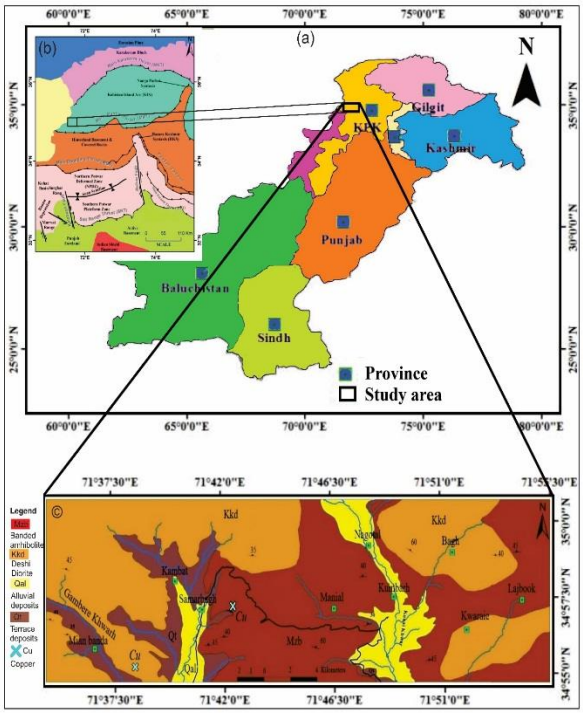

Fig. 1. Overview of research area (a) Pakistan map with provincial territories (b) Regional tectonic features of northern Pakistan (c) Represents the geological map of investigated region.

Materials and Methods

For the present study the data were collected in three stages i) Acquisition of remote sensing data, ii) Field observation, iii) laboratory analysis. The Landsat-7 data (151/36 path/row, acquired on 05 December 2017) of the selected spot of the Dir area. Additionally, Landsate-8 and Sentinel-2B data, with an acquisition date of 5 December 2017 were utilized for the designated area. The satellite imagery was geometrically and radiometrically corrected. During the field observation, alternative ground control points from topographic sheets and GPS-marked sites were used to geometrically rectify the remote sensing data. The radiometric adjustment was carried out (Chander et al., 2009), with corrected Digital Numbers (DNs) being converted to Top-Of-Atmosphere (TOA) reflectance. A Field Spec® Pro, Portable Spectro Radiometer was used to acquire the spectral data of (mineralized/ altered) samples collected from the study area.

The spectrometer has a sampling interval of 2 to 3 nm with a 'full' spectral range of 350-2500 nm. The spectrometer has sufficiently fast scan time of 100 milliseconds for a complete 350–2500 nm spectrum which helps to avoid errors in collecting the spectra while examining the samples. To process and interpret, principal component analysis (PCA) (Singh and Harrison, 1985) was applied over Landsat-7, Landsat-8 and sentinel-2B data to highlight the alteration zones in this area. Crosta approach (Crosta and Moore, 1989), a principal component analysis-based technique that used a combination of four bands 1, 4, 5, and 7 for hydroxyl-mineral discrimination and bands 1, 3, 4, and 5 for iron oxides minerals to analyse Landsat-7 data, was used to designate the zones of alteration. The Principal component analysis (PCA) technique was employed for two sets of band combinations; 2, 4, 5, 6 for iron-oxide minerals and bands 2, 5, 6, 7 for hydroxyl minerals of Landsat-8 to define the alteration zones (Crosta and Moore, 1990; Safari et al., 2018). Two sets of band combination 2, 4, 8, 11 and 2, 8, 11, 12 of Sentinel-2B were subjected to the same principal component analysis (PCA) techniques.

Results and Discussion

Landsat-7

The Crosta method, also known as feature-oriented principal component collection, has been extensively used in mineral research to pinpoint features of carbonate bearing minerals, hydroxyl minerals, and iron oxides minerals (Aydal et al., 2007; Ranjbar et al., 2004, Liu et al., 2013). Tables 1 and 2 show the PCA eigenvector values. In table 1, PC4 exhibits iron oxide crystals in bright pixels in bands 1 and 3, with an eigenvector value of 0.800 in band 1 and a negative eigenvector value of -0.583 in band 3. The hydroxyl minerals are highlighted as dark pixels in Table 2 PC4, with a negative eigenvector value (-0.607) at band 5

and a positive eigenvector value (0.661) at band 7. The RGB image uses the light pink pixels to represent iron oxide minerals as shown in (Fig. 3), and the same is highlighted in deep red pixels in (Fig. 4).

Table 1. Principal component analysis of bands 1, 3, 4, and 5 for iron minerals.

Iron-oxide PCA	PC1	PC2	PC3	PC4
B1	0.201	-0.159	0.540	**0.800**
B3	0.471	-0.246	0.613	-0.583
B4	0.468	0.882	0.028	0.036
B5	0.718	-0.368	-0.574	0.132

Table 2. Principal component analysis of bands 1, 4, 5, and 7 for hydroxyl minerals.

Hydroxyl PCA	PC1	PC2	PC3	PC4
B1	0.155	-0.136	-0.916	-0.342
B4	0.377	0.867	-0.168	0.277
B5	0.709	-0.046	0.354	**-0.607**
B7	0.573	-0.476	-0.079	**0.661**

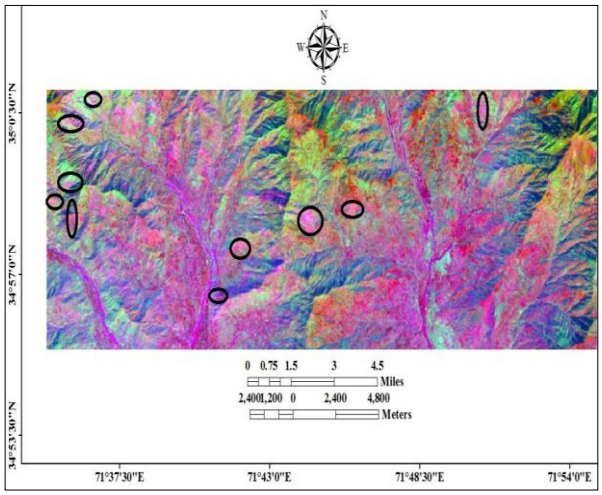

Fig. 3 Landsat-7 PCA with bands 1, 3, 4, 5 displayed as red, green, blue colour. A pink colour pixel shows iron alteration, circled with black line in the study area.

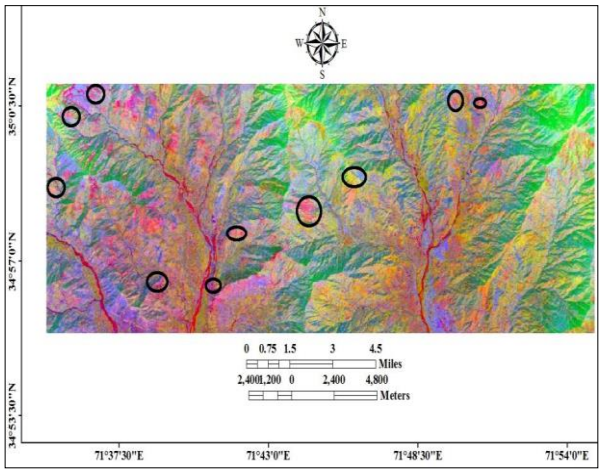

Fig. 4 Landsat-7 PCA with bands 1, 4, 5, 7 displayed as red, green, blue colour. Reddish pixels show hydroxyl alteration.

Landsat-8

Principal component analysis (PCA) techniques were used to process Landsat-8 images for the identification of alteration minerals (Tangestani and Moore, 2001). PCA technique was employed for two sets of band combination: 2, 4, 5, 6 and 2, 5, 6, 7 bands. The same methods used by (Osinowo et al., 2021) for the delineation of alteration zones and lithological mapping. PC4 highlighted iron-oxide minerals in bright pixels, as seen in bands 2 and 4, with positive eigenvector value of 0.800 for band 2 and a negative eigenvector value of -0.586 for band 4 in Table 3. PC4 appears to have mapped hydroxyl minerals in dark pixels detected in Band 6 with a negative eigenvector value of -0.459 compared to band 7 with a positive eigenvector value of 0.565 in the same PCA, as shown in Table 4. The reddish pixel observed on the RGB reflects iron oxide minerals as shown in (Fig. 6.).

Table. 3. Principal component analysis of bands 2, 4, 5, and 6 for iron minerals.

Iron-oxide PCA	PC1	PC2	PC3	PC4
B2	0.142	-0.137	0.561	**0.803**
B4	0.336	-0.256	0.691	**-0.586**
B5	0.620	0.783	0.691	0.020
B6	0.693	-0.548	-0.455	0.100

Table 4. Principal component analysis of bands 2, 5, 6, and 7 for hydroxyl minerals.

Hydroxyl PCA	PC1	PC2	PC3	PC4
B2	0.108	-0.095	-0.732	-0.665
B5	0.479	0.841	-0.187	0.162
B6	0.681	-0.179	0.541	**-0.459**
B7	0.542	-0.500	-0.368	**0.565**

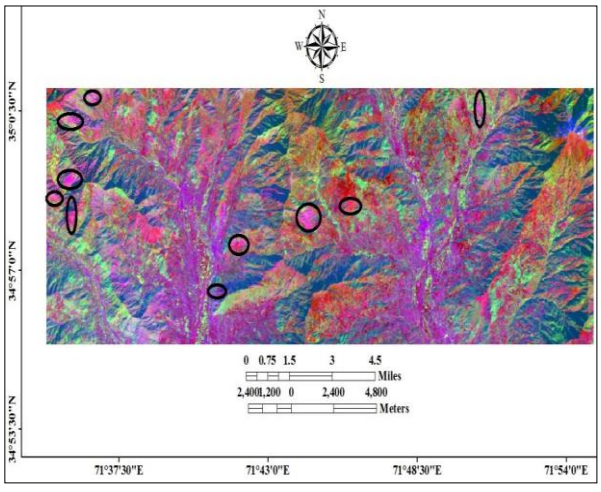

Fig. 5. Landsat-8 PCA with bands 2, 4, 5, 6 displayed as red, green, blue colour. Pinkish pixels show iron alteration in the study area.

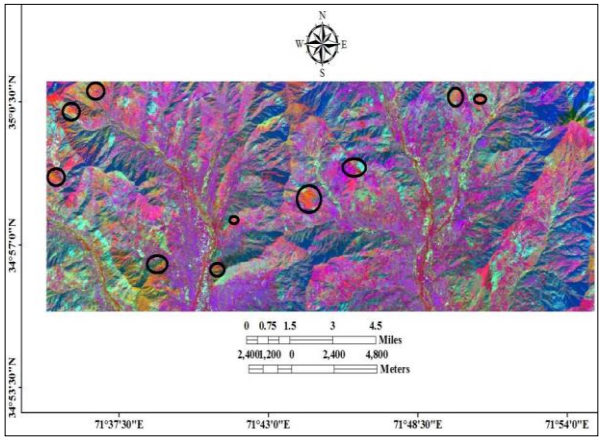

Fig. 6. Landsat-8 PCA with bands 2, 5, 6, 7 displayed as red, green, blue colour. Red pixels show hydroxyl alteration.

Sentinel-2B

Principal component analysis (PCA) approaches were used on two sets of band combinations: 2, 4, 8, 11 and 2, 8, 11, 12 (Crosta and Moore, 1990; Safari et al., 2018; Tangestani and Moore, 2001; Liu et al., 2011). PC4 demarcate iron-oxide minerals in bright pixels as seen in Bands 2 and 4, which have a high eigenvector value of (0.824) at band 2 and a negative eigenvector value of (-0.555) at band 4 in Table. 5. Whereas mapped hydroxyl minerals in dark pixels as shown in Table 6. By observing the same PCA, Band 11 demarcate a larger eigenvector value (-0.580) than Band 12 with a lower eigenvector value of (0.631). Iron oxide minerals are highlighted in yellow pixel over RGB image (Fig. 7) while hydroxyl minerals are demarcated as a reddish pixel in (Fig. 8).

Table 5. Principal component analysis of bands 2, 4, 8, and 11 for iron minerals.

Iron-oxide PCA	**PC1**	**PC2**	**PC3**	**PC4**
B2	0.142	0.079	-0.541	**0.824**
B4	0.313	0.254	-0.726	**-0.555**
B8	0.553	-0.831	-0.027	-0.033
B11	0.758	0.486	0.422	0.099

Table 6. Principal component analysis of bands 2, 8, 11, and 12 for hydroxyl minerals.

Hydroxyl PCA	**PC1**	**PC2**	**PC3**	**PC4**
B2	0.056	0.007	-0.870	-0.488
B8	0.477	0.862	-0.051	0.160
B11	0.682	-0.247	0.367	**-0.580**
B12	0.550	-0.441	-0.322	**0.631**

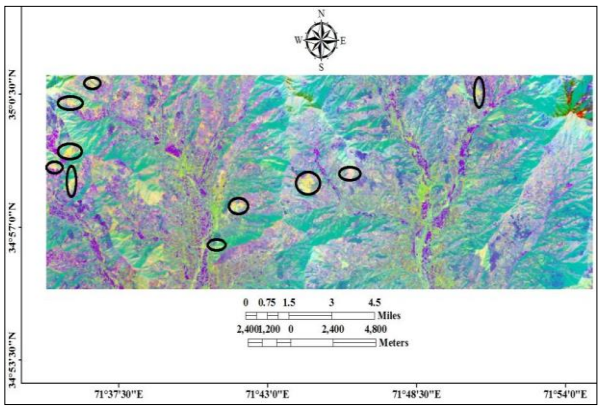

Fig. 7. Sentinel-2B PCA with bands 2, 4,8,11 displayed as red, green, blue colour. Deep yellow pixels show iron alteration in the study area.

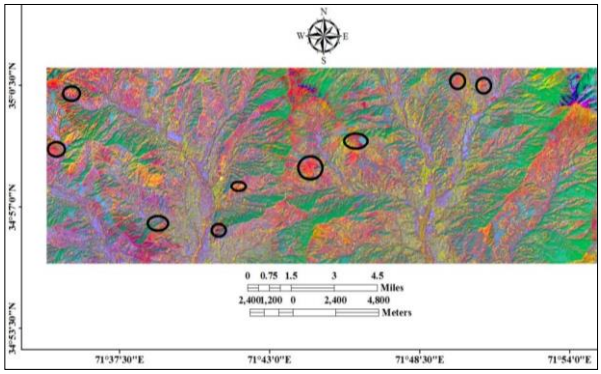

Fig. 8. Sentinel-2B PCA with bands 2, 8, 11, 12 displayed as red, green, blue colour. Red pixels show hydroxyl alteration in the study area.

Ground truth observation

For the confirmation of the remote sensing results on the ground, field investigation was carried out in August 2019. The checkpoints were noted with GPS, zones of alteration were identified and sixteen samples were collected from the delineated zones. The collected samples were processed in the laboratory for petrographic and spectrometric analysis. Various alteration features were observed in the field such as chloritization and sericitization along the contact zones of the host rock. Mineralization were also seen along these alteration zones (Figs. 9, 10)

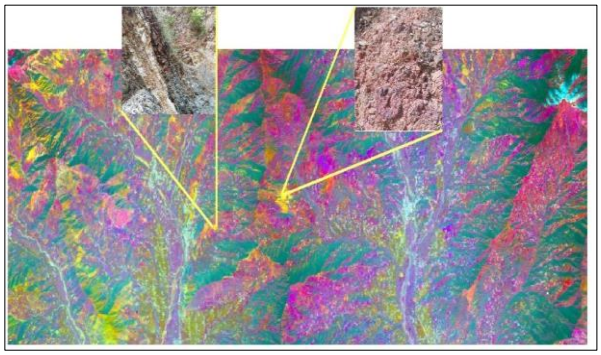

Fig. 9. Map shows the spots of mineralization that were marked by remote sensing techniques.

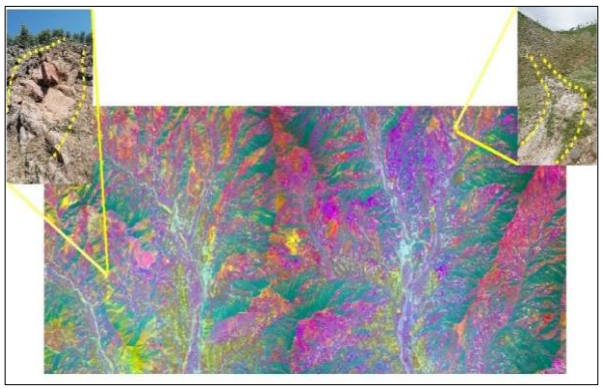

Fig. 10. Map shows the locations of mineralization that were marked by remote sensing techniques.

Spectrometry

For the spectrometric observations random samples were collected under names (JUG-2-3-4-5 and SUG-14-15) were checked by Portable Spectro Radiometer. The key alteration minerals muscovite, kaolinite chlorite, Sericite and illite containing Al-OH associated with hydroxyl mineralization are shown (Fig. 11). Goethite and hematite are the minerals associated with iron oxide anomalies containing Fe^{2+}, Fe^{3+}. Results delineate the various wavelengths, which display absorption and reflection characteristics. Goethite shows absorption at 400-900nm. Sericite is responsible for the huge decreasing spectral absorption function between 1400-2200nm, whereas chlorite shows the absorption function at 2200-2300 nm. Water content in the samples reflects absorption properties at 1900 nm (Fig. 11).

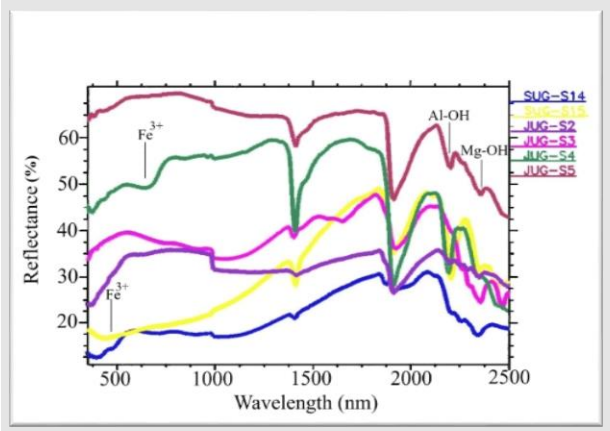

Fig. 11 Spectral reflectance of altered rocks, showing depths of absorption features for different minerals at various wavelengths.

Petrography

Furthermore, to confirm remote sensing results, petrography of selected samples was also carried out to determine the mineralogical composition and texture of the alteration minerals. Various key alteration minerals identified such as sericite, chlorite and ore minerals shows in (Fig. 11). The petrography of selected samples approves the hydrothermal alteration in the area and remote sensing results.

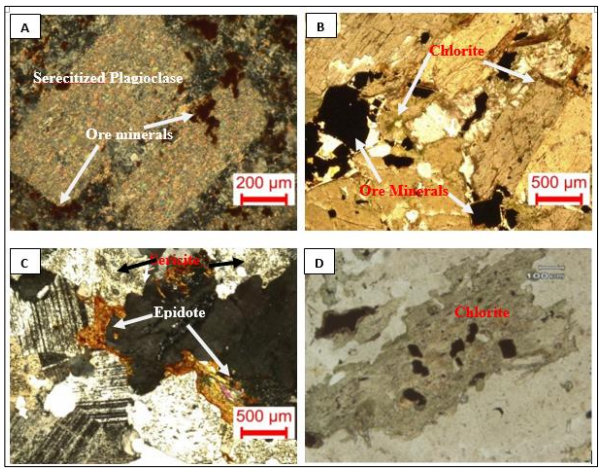

Fig. 12. Photomicrographs showing different alteration minerals from the study area.

Overall in this study we adopted the PCA techniques for remote sensing data coupled with the field observation, petrography and spectrometric analysis. A combination of PCA and Crosta techniques applied to Landsat-7, Landsat-8 and Sentinel-2B has led to the delineation of mineralized zones. The colour composites of PCA1, PCA2, PCA3 and PCA4 of Landsat-7, Landsat-8 and Sentinel-2B in RGB images displayed the zones of alteration present an investigated area in dissimilar colours. PCA techniques were applied to two sets of four bands of Landsat-7 data, mapped the zones of alteration effectively in the investigated area (Aydal et al., 2007, Liu et al., 2013) (Fig. 2, 3). Four bands of Landsat-8 data were subjected to PCA and marked the alteration zone (Fig. 4, 5). The (Osinowo et al., 2021) used the same method to delineate the zones of mineralization. Simulation of Landsat data utilized to select the bands of Sentinel-2B data for principal component analysis. Two sets of four bands were selected and subjected to PCA techniques for further analysis (Fig. 6, 7). The comparative methods of remote sensing data proved to be effectively discriminate the alteration zones in the study area.

The results obtained from Landsat-7, PCA with bands 1, 3, 4, 5 displayed as red, green, blue colour. A pink colour pixel shows iron alteration. Landsat-7 PCA with bands 1, 4, 5, 7 presented as red, green, blue colour whereas, reddish pixels show hydroxyl alteration in the study area. Followed by Landsat-8 PCA with bands 2, 4, 5, 6 exhibited as red, green, blue colour along with pinkish pixels show iron alteration. Landsat-8 PCA with bands 2, 4, 5, 6 and 2, 5, 6, 7 presented as grey colour and bright pixels showing iron (F) + hydroxyl (H) alteration in the study area. Sentinel-2B PCA with bands 2, 4,8,11 displayed as red, green, blue colour. Deep yellow pixels show iron alteration in the study area. Sentinel-2B PCA with bands 2, 4, 8, 11 and 2, 8, 11, 12 displayed as grey colour. Bight pixels show iron (F) + hydroxyl (H) alteration in the study area. Petrographic study was quite beneficial to confirm the alteration minerals at the marked alteration zones. The

spectrometric analysis displays the absorption features of various alteration minerals. The major alteration minerals observed with spectrometric analysis are sericite, chlorite and goethite (Fig. 11). Various alteration minerals were observed by studying the thin sections under the microscope that confirms the alteration zones in the area. These alteration minerals include iron oxides, chlorite, epidote, sericite etc. (Fig. 12).

Conclusion

For extensive geological mapping and minerals detection using remote sensing imageries in rugged and hilly terrains is an efficient, convenient and cost-effective approach. To save time and obtain the accurate results, the remote sensing PCA basis approach was adopted. This study determines the significance and benefits of the comparison of Landsat-7, Landsat-8 and Sentinel-2B remote sensing datasets in identifying alteration zones in the Dir area. The principal component analysis technique was used to mark zones of alteration in this study. These techniques were quite helpful for each dataset to demarcate the zones of alteration. Remote sensing data comparison method was found useful in mapping mineral resources in the study area. The marked alteration zones match well with the copper mineralization mined locally at places. Field investigation, petrography and spectrometry of the collected samples are the key studies after remote sensing data processing to confirm the results and zones of mineralization on the ground. PCA method has consistently demonstrated the accuracy and importance in geological discrimination and mineral exploration outcomes. The positive results produced by this technique lead us to employ it at various phases of the exploration and mineral prospecting process.

References

Abhary, A., Hassani, H. (2016). Mapping hydrothermal mineral deposits using PCA and BR methods in Baft 1: 100000 geological sheet, Iran. *International Journal of Advanced Engineering, Management and Science*, ***2(***9), 239620.

Ahmad, L. (2016). *Geologica,* Geochemical and remote sensing studies for identification of source rocks for gold in selected areas of Skardu and Astore, Northern Pakistan, (Doctoral dissertation, University of Peshawar).

Ahmad, M. N., Yoshida, M., Fujiwara, Y. (2000). Paleo-magnetic study of Utror Volcanic Formation: Re-magnetizations and post folding rotations in Utror area, Kohistan arc, northern Pakistan. *Earth, Planets and Space*, ***52,*** 425-436.

Amer, R., El Mezayen, A., Hasanein, M. (2016). ASTER spectral analysis for alteration minerals associated with gold mineralization. *Ore Geology Reviews*, ***75,*** 239-251.

Anwar, M., Abu El-Leil, I., Salem, S. M. (2023). Lithological and Alteration Mapping at the Um El-Rus Area, Central Eastern Desert, Egypt, Using Remote Sensing Techniques. *Journal of the Indian Society of Remote Sensing*, ***51***(4), 829-848.

Aydal, D., Arda1, E., Dumanlilar, Ö. (2007). Application of the Crosta technique for alteration mapping of granitoidic rocks using ETM+ data: case study from eastern Tauride belt (SE Turkey). *International Journal of Remote Sensing*, ***28***(17), 3895-3913.

Bignold, S. M., & Treloar, P. J. (2003). Northward subduction of the Indian Plate beneath the Kohistan island arc, Pakistan Himalaya: new evidence from isotopic data. *Journal of the Geological Society*, ***160***(3), 377-384.

Chander, G., Markham, B. L., Helder, D. L. (2009). Summary of current radiometric calibration coefficients for Landsat MSS, TM, ETM+, and EO-1 ALI sensors. *Remote sensing of environment*, ***113***(5), 893-903.

Corumluoglu, O., Vural, A., Asri, I. (2015). Determination of Kula basalts (Geosite) in Turkey using remote sensing techniques. *Arabian Journal of Geosciences*, **8,** 10105-10117.

Crosta, A. P. (1989). Enhancement of Landsat Thematic Mapper imagery for residual soil mapping in SW Minas Gerais State Brazil, a prospecting case history in greenstone belt terrain. In *Proceedings of the 7^< th> ERIM Thematic Conference on Remote Sensing for Exploration Geology, 1989*.

Crosta, A. P., Sabine, C., Taranik, J. V. (1998). Hydrothermal alteration mapping at Bodie, California, using AVIRIS hyperspectral data. *Remote Sensing of Environment*, ***65***(3), 309-319.

Ducart, D. F., Silva, A. M., Toledo, C. L. B., Assis, L. M. D. (2016). Mapping iron oxides with Landsat-8/OLI and EO-1/Hyperion imagery from the Serra Norte iron deposits in the Carajás Mineral Province, Brazil. *Brazilian Journal of Geology*, ***46,*** 331-349.

El Atillah, A., El Morjani, Z. E. A., Souhassou, M. (2019). Use of the sentinel-2A multispectral image for litho-structural and alteration mapping in Al Glo'a map sheet (1/50,000) (Bou Azzer–El Graara Inlier, Central Anti-Atlas, Morocco). *Artificial Satellites*, ***54***(3), 73-96.

Ferrier, G., White, K., Griffiths, G., Bryant, R., Stefouli, M. (2002). The mapping of hydrothermal

alteration zones on the island of Lesvos, Greece using an integrated remote sensing dataset. *International Journal of Remote Sensing*, ***23*** (2), 341-356.

Fraser, S. J. (1991). Discrimination and identification of ferric oxides using satellite Thematic Mapper data: A Newman case study. *International Journal of Remote Sensing*, ***12***(3), 635-614.

Gabr, S. S., Hassan, S. M., Sadek, M. F. (2015). Prospecting for new gold-bearing alteration zones at El-Hoteib area, South Eastern Desert, Egypt, using remote sensing data analysis. *Ore Geology Reviews*, ***71,*** 1-13.

Gahlan, H., Ghrefat, H. (2018). Detection of gossan zones in arid regions using Landsat 8 OLI data: Implication for mineral exploration in the eastern Arabian Shield, Saudi Arabia. *Natural Resources Research*, ***27***, 109-124.

Han, L., Song, T., Zhang, R. (2010, December). Extraction of mineralized alteration information based on remote sensing in western Tianshan, Xinjiang. In *2010 2nd International Conference on Information Engineering and Computer Science*, 1-4.

Hunt, G. R. (1977). Spectral signatures of particulate minerals in the visible and near infrared. *Geophysics*, ***42***(3), 501-513.

Khan, S. D., Glenn, N. F. (2006). New strike-slip faults and litho-units mapped in Chitral (N. Pakistan) using field and ASTER data yield regionally significant results. *International Journal of Remote Sensing*, ***27***(20), 4495-4512.

Linhai Jing, Q. C., Panahi, A. (2006). Principal component analysis with optimum order sample correlation coefficient for image enhancement. *International Journal of Remote Sensing*, ***27***(16), 3387-3401.

Liu, C., Qiu, C., Wang, L., Feng, J., Wu, S., Wang, Y. (2023). Application of ASTER Remote Sensing Data to Porphyry Copper Exploration in the Gondwana Region. *Minerals*, ***13***(4), 501.

Liu, L., Zhou, J., Jiang, D., Zhuang, D., Mansaray, L. R., Hu, Z., Ji, Z. (2016). Mineral resources prospecting by synthetic application of TM/ETM+, Quickbird and Hyperion data in the Hatu area, West Junggar, Xinjiang, China. *Scientific Reports*, ***6*(**1), 21851.

Liu, L., Zhuang, D. F., Zhou, J., Qiu, D. S. (2011). Alteration mineral mapping using masking and Crosta technique for mineral exploration in mid-vegetated areas: a case study in Areletuobie, Xinjiang (China). *International Journal of Remote Sensing*, ***32***(7), 1931-1944.

Liu, L., Zhou, J., Jiang, D., Zhuang, D., Mansaray, L.R., Zhang, B. (2013). Targeting mineral resources with remote sensing and field data in the Xiemisitai area, West Junggar, Xinjiang, China. *Remote Sensing*, ***5***(7), 3156-3171.

Mars, J. C., Rowan, L. C. (2010). Spectral assessment of new ASTER SWIR surface reflectance data products for spectroscopic mapping of rocks and minerals. *Remote Sensing of Environment*, ***114***(9), 2011-2025.

Masoumi, F., Eslamkish, T., Honarmand, M., Abkar, A. A. (2017). A comparative study of landsat-7 and landsat-8 data using image processing methods for hydrothermal alteration mapping. *Resource Geology*, ***67***(1), 72-88.

Mia, B., Fujimitsu, Y. (2012). Mapping hydrothermal altered mineral deposits using Landsat 7 ETM+ image in and around Kuju volcano, K*1*yushu, Japan. *Journal of Earth System Science*, ***121***, 1049-1057.

Michael, P. C., David, C. R. (1986). Collision tectonics in the NW Himalayas. *Geological Society, London, Special Publications*, ***9***(1), 203-219.

Moore, F., Rastmanesh, F., Asadi, H., Modabberi, S. (2008). Mapping mineralogical alteration using principal-component analysis and matched filter processing in the Takab area, north-west Iran, from ASTER data. *International Journal of Remote Sensing*, ***29***(10), 2851-2867.

Osinowo, O.O., Gomy, A.,Isseini, M. (2021). Mapping hydrothermal alteration mineral deposits from Landsat 8 satellite data in Pala, Mayo Kebbi Region, Southwestern Chad. *Scientific African*, *11*, p.e00687.

Ousmanou, S., Fozing, E. M., Kwékam, M., Fodoue, Y., Jeatsa, L. D. A. (2023). Application of remote sensing techniques in lithological and mineral exploration: discrimination of granitoids bearing iron and corundum deposits in southeastern Banyo, Adamawa region-Cameroon. *Earth Science Informatics*, 1-27.

Pirajno, F., Pirajno, F. (1992). Greisen systems. *Hydrothermal Mineral Deposits: Principles and Fundamental Concepts for the Exploration Geologist*, 280-324.

Pour, A. B., Hashim, M. (2015). Hydrothermal alteration mapping from Landsat-8 data, Sar Cheshmeh copper mining district, south-eastern Islamic Republic of Iran. *Journal of Taibah University for Science*, ***9***(2), 155-166.

Ranjbar, H., Honarmand, M., Moezifar, Z. (2004). Application of the Crosta technique for porphyry copper alteration mapping, using ETM+ data in

the southern part of the Iranian volcanic sedimentary belt. *Journal of Asian Earth Sciences*, ***24***(2), 237-243.

Sabins, F. F. (1999). Remote sensing for mineral exploration. *Ore Geology Reviews*, ***14***(3-4), 157-183.

Sadeghi, B., Khalajmasoumi, M., Afzal, P., Moarefvand, P., Yasrebi, A. B., Wetherelt, A., Ziazarifi, A. (2013). Using ETM+ and ASTER sensors to identify iron occurrences in the Esfordi 1: 100,000 mapping sheet of Central Iran. *Journal of African Earth Sciences*, ***85***, 103-114.

Safari, M., Maghsoudi, A., Pour, A. B. (2018). Application of Landsat-8 and ASTER satellite remote sensing data for porphyry copper exploration: a case study from Shahr-e-Babak, Kerman, south of Iran. *Geocarto International*, ***33***(11), 1186-1201.

Sekandari, M., Masoumi, I., Beiranvand Pour, A., M Muslim, A., Rahmani, O., Hashim, M., Aminpour, S. M. (2020). Application of Landsat-8, Sentinel-2, ASTER and WorldView-3 spectral imagery for exploration of carbonate-hosted Pb-Zn deposits in the Central Iranian Terrane (CIT). *Remote Sensing*, ***12***(8), 1239.

Shah, M. T., Shervais, J. W. (1999). The Dir-Utror metavolcanic sequence, Kohistan arc terrane, northern Pakistan. *Journal of Asian Earth Sciences*, ***17***(4), 459-475.

Shoulin, Z. H. A. N. G., Shuixing, F. U., Chunxia, L. I. (2004). Remote sensing geological exploration model for copper and gold deposits in the east Tianshan, Xinjiang. *Acta Geologica Sinica-English Edition*, ***78***(2), 423-427.

Sikakwe, G. U. (2023). Mineral exploration employing drones, contemporary geological satellite remote sensing and geographical information system (GIS) procedures: A review. *Remote Sensing Applications: Society and Environment*, 100988.

Singh, A., Harrison, A. (1985). Standardized principal components. *International Journal of Remote Sensing*, ***6(***6), 883-896.

Sullivan, M. A., Windley, B. F., Saunders, A. D., Haynes, J. R., Rex, D. C. (1993). A paleo-geographic reconstruction of the Dir Group: Evidence for magmatic arc migration within Kohistan, N. Pakistan. *Geological Society, London, Special Publications*, ***74***(1), 139-160.

Tahirkheli, R. K. (1979). Geology of Kohistan and adjoining Eurasian and Indo-Pakistan continents, Pakistan. *Geol. Bull. Univ. Peshawar*, ***11***(1), 1-30.

Tahirkheli, R. K. (1982). Geology of the Himalaya, Karakoram and Hindukush in Pakistan. *Geological Bulletin, University of Peshawar*, ***15,*** 1-51.

Tangestani, M. H., Moore, F. (2001). Comparison of three principal component analysis techniques to porphyry copper alteration mapping: a case study, Meiduk area, Kerman, Iran. *Canadian Journal of Remote Sensing*, ***27***(2), 176-182.

Torres-Vera, M. A., Prol-Ledesma, R. M. (2003). Spectral enhancement of selected pixels in Thematic Mapper images of the Guanajuato district (Mexico) to identify hydrothermally altered rocks. *International Journal of Remote Sensing*, ***24***(22), 4357-4373.

Vural, A., Corumluoglu, Ö., Asri, I. (2017). Remote sensing technique for capturing and exploration of mineral deposit sites in Gumushane metallogenic province, NE Turkey. *Journal of the Geological Society of India*, ***90,*** 628-633.

Yousufi, A., Ahmadi, H., Bekbotayeva, A., Arshamov, Y., Baisalova, A., Omarova, G., Pekkan, E. (2023). Integration of remote sensing and field data in ophiolite investigations: A case study of Logar ophiolite complex, SE Afghanistan. *Minerals*, ***13***(2), 234.

Zhang, B. P., Zhang, Y. M. (2007). Application of remote sensing alteration information extraction to copper and iron deposit exploration in Banchangou region, western Tianshan. *Resour. Geol*, ***21,*** 90-93.